Geomorphology 138 (2012) 189–202

Contents lists available at SciVerse ScienceDirect

Geomorphology

journal homepage: www.elsevier.com/locate/geomorph

Probability maps of landslide reactivation derived from tree-ring records: Pra Bellon landslide, southern French Alps

Jérôme Lopez Saez [a,*], Christophe Corona [a], Markus Stoffel [b,c], Philippe Schoeneich [d], Frédéric Berger [a]

[a] Cemagref UR EMGR, 2 rue de la papeterie, BP 76 F-38402 Saint-Martin d'Hères Cedex, France
[b] Laboratory of Dendrogeomorphology (dendrolab.ch), Institute of Geological Sciences, University of Bern, Baltzerstrasse 1 +3, CH-3012 Bern, Switzerland
[c] Climatic Change and Climate Impacts, Institute for Environmental Sciences, University of Geneva, 7, chemin de Drize, CH-1227 Carouge-Geneva, Switzerland
[d] Institut de Géographie Alpine, Laboratoire Politiques publiques, Action Politique, Territoires (PACTE) UMR 5194 du CNRS, Université Joseph Fourier, 14 bis avenue Marie Reynoard, 38 100 Grenoble, France

ARTICLE INFO

Article history:
Received 26 May 2011
Received in revised form 24 August 2011
Accepted 31 August 2011
Available online 14 September 2011

Keywords:
Dendrogeomorphology
Landslide return period
Poisson distribution model
Probability maps

ABSTRACT

Probability maps of landslide reactivation are presented for the Pra Bellon landslide located in the southern French Alps based on results obtained with dendrogeomorphic analysis. Spatiotemporal patterns of past landslide activity was derived from tree-ring series of 403 disturbed mountain pine trees growing in the landslide body. In total, 704 growth disturbances were identified in the samples indicating 22 reactivation phases of the landslide body between 1910 and 2011. The mean return period was 4.5 years. Given the spatiotemporal completeness of the reconstruction, probabilities of landslide reactivation were computed and illustrated using a Poisson distribution model and for 5, 20, 50, and 100 years. Probability of landslide reactivation is highest in the central part of the landslide body and increases from 0.13 for a 5-year period to 0.94 for a 100-year period. Conversely, probabilities of reactivation are lower at its margins. The proposed method differs from conventional approaches based on statistical analyses or physical modeling that have demonstrated to have limitations in the prediction of spatiotemporal reactivation of landslides. Our approach is, in contrast, based on extensive data on past landslides and therefore allowed determination of quantitative probability maps of reactivation derived directly from the frequency of past events. This approach is considered a valuable tool for land managers in charge of protecting and forecasting people and their assets from the negative effects of landslides as well as for those responsible for land use planning and management. It demonstrates the reliability of dendrogeomorphic mapping that should be used systematically in forested shallow landslides.

1. Introduction

Each year, mass movements cause considerable financial damage to alpine societies (Hilker et al., 2009). They repeatedly destruct settlements, disrupt transportation corridors, or even lead to the loss of life. Global statistics show that damage from landslides has risen for the last 30 years in mountain areas (Alexander, 2008). This trend is linked both to an increase in the occurrence of hazardous events and to larger populations living in constantly growing Alpine settlements (Petrascheck and Kienholz, 2003). In addition, extensive records of landslide activity (Guzzetti et al., 1994; Floris and Bozzano, 2008) show that new slides are, in many cases, consequent upon partial or complete reactivation of existing landslide bodies. A need therefore exists for the documentation of past events and elaboration of site-specific landslide reactivation maps indicating the degree of stability of specific areas as well as providing information on the probability of landslide reactivation (Varnes, 1984).

Methods available for the assessment of probabilities of landslide reactivation have been reviewed by Aleotti and Chowdhury (1999). In the past, two independent approaches have been traditionally used: (i) analysis of the potential for slope failure and (ii) a statistical treatment of past landslide events. The first approach takes account of present slope conditions and evaluates the potential for instability (e.g., Corominas and Moya, 2008). The second approach, which is in line with the objectives of this paper, obviates the causes of instability and analyses the frequency of past events, considered to be repetitive, to derive probabilities of reactivation (Brabb, 1984).

As complete as possible landslide records covering multiple decades are normally needed to perform a reliable probabilistic analysis, but such data is not normally available with satisfying spatial resolution over long enough timescales and as a continuous record (Claessens et al., 2006; Thiery et al., 2007; Corominas and Moya, 2008). Estimates were derived from archives such as narrations, paintings, engravings and other artwork, terrestrial or aerial photographs, remote sensing series, or incidental statements (Brunsden et al., 1976; Hovius et al., 1997;

* Corresponding author.
E-mail addresses: jerome.lopez@cemagref.fr, jerome.lopezsaez@gmail.com (J. Lopez Saez).

0169-555X/$ – see front matter © 2011 Elsevier B.V. All rights reserved.
doi:10.1016/j.geomorph.2011.08.034

Martin et al., 2002). The temporal window of the record seldom spans more than a few decades and rarely covers centuries. In addition and even more importantly, archival data on landslides usually lack spatial completeness, resolution, and precision and invariably emphasize events that caused damage to human structures. At the same time, they tend to underestimate failures, even large ones that took place in areas that have been unpopulated in the past (Guzzetti et al., 1994; Ibsen and Brunsden, 1996; Carrara et al., 2003).

In order to compute accurate probability maps of landslide reactivation at the local scale, available for disaster prevention and generation of risk maps, an approach is thus required that offers both an adequate temporal and spatial resolution. On shallow landslide bodies covered with tree stands, dendrogeomorphology may allow such a reconstruction of landslide reactivation with the desired resolution through the analysis of growth disturbances contained in tree-ring records (Alestalo, 1971; Stoffel et al., 2010). Indeed, trees suffering from superficial and slow movements may survive reactivation events and conserve evidence of topping, tilting (or S-shaped stems), scarring, or root breakage in their increment rings (Carrara and O'Neill, 2003; Stefanini, 2004). As tree-ring series provide a continuous record over the lifespan of the tree and, collectively, over the lifespan of the sampled population (Procter et al., 2011), they offer a unique spatiotemporal resolution of past activity. Nevertheless, no attempts have been undertaken so far to use the spatial distribution of disturbed trees as a source of information for the quantification and mapping of probabilities of future landslide reactivation.

The purpose of this study therefore is to map the probability of landslide reactivation for a site in the Ubaye valley (French Alps) using dendrogeomorphic techniques. Through an exhaustive sampling of 403 mountain pines (*Pinus uncinata* Mill. ex Mirb), we (i) reconstruct a chronology of past landslide reactivations; (ii) evaluate its accuracy and compare the data with historical archives; (iii) determine the spatial extent of past events; (iv) derive a high resolution landslide return period map; and finally (v) quantify and map the probability of landslide reactivation for the coming 5, 20, 50, and 100 years using a Poisson distribution model.

2. Study site

The Pra Bellon landslide (44°25′ N., 6°37′ E.; Fig. 1A) is located in the Riou-Bourdoux catchment, a tributary of the Ubaye River and on the north-facing slope of the Barcelonnette basin, 3 km north of Saint-Pons (Alpes de Haute-Provence, France). The Riou-Bourdoux catchment has been considered the most hazardous area in France (Delsigne et al., 2001) and is well known for its extensive mass movement activity. The history of hydrogeomorphic processes in the wider case-study area has been documented extensively (Braam et al., 1987), and activity seems to date back to at least the fifteenth century

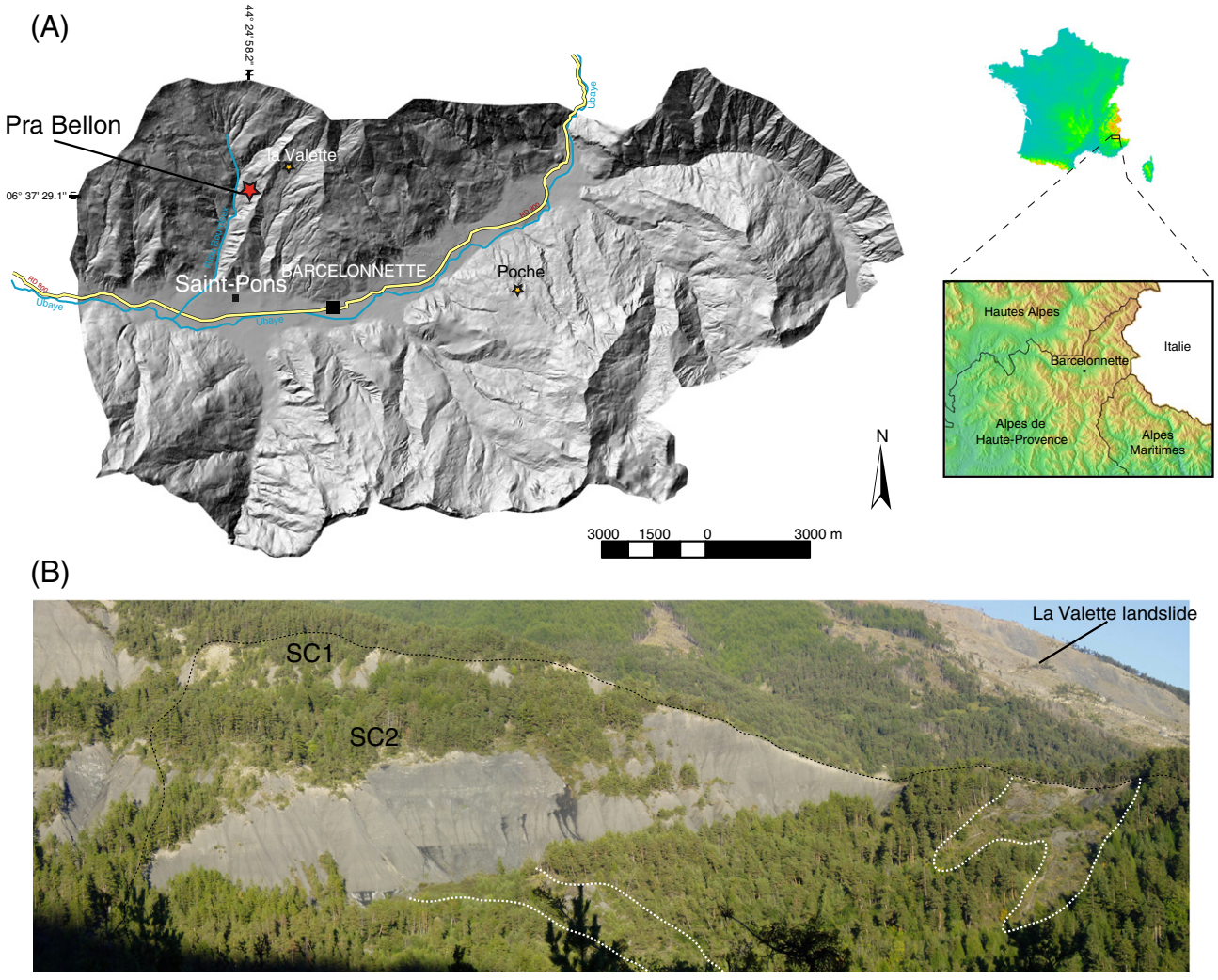

Fig. 1. (A) The Pra Bellon landslide is located in the southern French Alps, in the Ubaye valley, near the village of Saint-Pons. (B) View of the two mains scarps (SC1 and SC2) and of the landslide body. The black dotted line delimits the landslide area. The white dotted line delineates two recent earthflows.

when the area was almost completely deforested (Weber, 1994). Restoration activities in the Riou-Bourdoux catchment started in 1868 and are still ongoing under the supervision of the RTM services (Flez and Lahousse, 2003). Extensive records of debris flow activity exist for the Pra Bellon catchment, but conversely, for the Pra Bellon landslide, only one landslide event has been inventoried in spring 1971 (Delsigne et al., 2001).

The Pra Bellon landslide is 175 m long, 450 m wide (32 ha), and has a depth varying between 4 and 9 m. Its elevation ranges from 1470 to 1750 m asl and the volume of the body has been estimated at 1.5–2×10^6 m^3 (Weber, 1994; Stien, 2001). The rotational landslide is a slump characterized by a 1.5-m-thick top moraine layer underlain by a weathered and unsaturated black marl layer (thickness 5–6 m), which overlies bedrock of unweathered marl (Mulder, 1991). Colluvium consists of 60–80% silt, 10–35% clay, and 0–10% sand (Mulder, 1991) and is very sensitive to mass movement (Antoine, 1995; Meunier et al., 1995). In dry conditions, black marls are quite solid and able to absorb large quantities of water, but soften considerably when wet. Landslide activity at Pra Bellon was considered the consequence of (i) a discontinuity between the moraine deposits and black marls favoring slope movements (Dehn and Buma, 1999); (ii) high groundwater levels in the weathered marl layer and the temporal occurrence of a perched water table in the top moraine deposits (Caris and van Asch, 1991); (iii) microtectonics, forming a potential sliding surface and guiding fragmentation and weathering (Maquaire et al., 2003).

The study site is characterized by irregular topography with a mean slope angle of about 20°. Two main scarps (SC) delineate the head of the landslide (Fig. 1B): SC1, located at around 1720 m asl, is 3 m high and partly colonized by trees; SC2, located at around 1640 m asl, is 20 m high, with a slope angle of 70°, and completely void of vegetation. On the landslide body, four recent earthslides and several minor internal scarps and cracks are clearly visible and presented in Fig. 1.

P. uncinata has a competitive advantage on these dry, matrix-poor soils (Dehn and Buma, 1999; Fig. 1B) and form nearly homogeneous forest stands outside the surfaces affected by the scarps and recent earthflows. The tilted and deformed *P. uncinata* trees also clearly indicate that the Pra Bellon landslide has been affected by multiple reactivations in the past.

The climate at the study site is dry and Mediterranean with strong interannual rainfall variability. According to the HISTALP data set (Efthymiadis et al., 2006), precipitation at the gridded point closest to the Pra Bellon landslide (44°25′ N., 6°35′ E.) is 895 ± 154 mm. $year^{-1}$ for the period 1800–2003. Rainfall can be violent, with intensities exceeding 50 mm h^{-1}, especially during frequent summer storms (Flageollet, 1999). Mean annual temperature is 7.5 °C with 130 days of freezing per year (Maquaire et al., 2003).

3. Material and methods

3.1. Reconstruction of landslide events with tree-ring series

Dendrogeomorphic techniques have been used to date landslide events in several ways. Tree age may supply a first but important

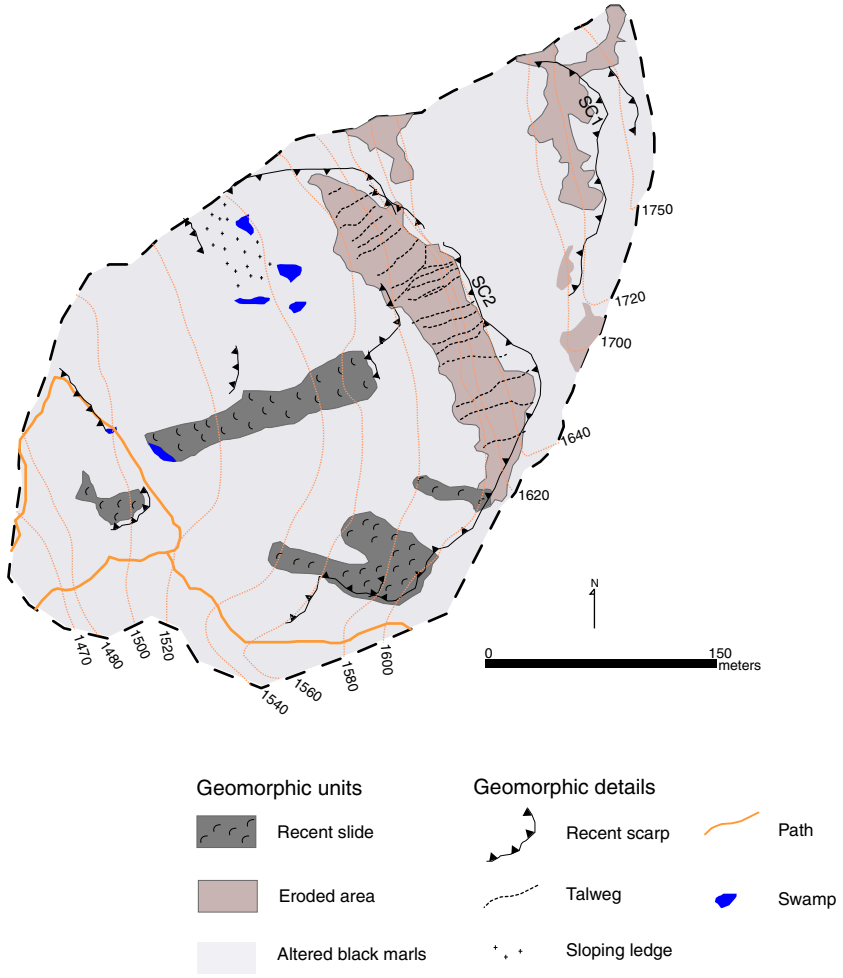

Fig. 2. Geomorphic map.
Adapted from Utasse (2009), and modified after personal observations.

information as the oldest undisturbed tree on a landslide body will provide a minimum age of movement (Carrara and O'Neill, 2003). The approach using tree age on landslide surfaces is not new and extends back to the late nineteenth century when McGee (1893) and Fuller (1912) aged movements in Tennessee and along the Mississippi River.

A more complex analysis of landslide movement involves the interpretation of growth disturbances in annual ring series of trees affected by landslide activity (Carrara and O'Neill, 2003). The earliest dendrogeomorphic studies of landslides date back to Alestalo (1971), and the method has been used ever since extensively in the United States (e.g., Reeder, 1979; Hupp, 1983; Osterkamp et al., 1986; Williams et al., 1992; Carrara and O'Neill, 2003), in Canada (Butler, 1979), but also in Quebec (Bégin and Filion, 1988). In Europe, tree rings have been used to reconstruct the frequency and landslides reactivation in the French (Braam et al., 1987; Astrade et al., 1998) and Italian Alps (Fantucci and McCord, 1995; Fantucci and Sorriso-Valvo, 1999; Santilli and Pelfini, 2002; Stefanini, 2004), in the Spanish Pyrenees (Corominas and Moya, 1999), and in the Flemish Ardennes (Belgium; Van Den Eeckhaut et al., 2009).

3.2. Collection and preparation of samples

Analysis of past landslide activity started with the geomorphic mapping (Fig. 2) where geomorphic units were combined with geomorphic details associated with past activity. The map was realized on the basis of previous work (Stien, 2001; Utasse, 2009) and with the help of a detailed GPS field survey.

Based on an outer inspection of the stem, *P. uncinata* trees obviously influenced by past landslide activity were sampled. Normally, four cores per tree were extracted: two in the supposed direction of landslide movement (i.e., upslope and downslope cores) and two perpendicular to the slope. To gather the greatest amount of data on past events, trees were sampled within the tilted segment of the stems. To avoid misinterpretation, trees growing in sectors influenced by processes other than landslide or anthropogenic activity (sylviculture) were disregarded systematically for analysis.

A total of 403 *P. uncinata* trees (Fig. 3) were sampled with 1563 increment cores. For each tree, additional data were collected including (i) tree height; (ii) diameter at breast height (DBH); (iii) visible defects in tree morphology, and particularly the number of knees; (iv) position of the extracted sample on the stem; and (v) photographs of the entire tree. The GPS coordinates with <1 m accuracy were recorded for each tree sample using a Trimble GeoExplorer. In addition, 20 undisturbed trees located above SC1 and showing no signs of landslide activity or other geomorphic processes were sampled to build a reference chronology. Two cores per tree were extracted in this case parallel to the slope direction and systematically at breast height. This reference chronology represents common variations of tree growth at the site (Cook and Kairiukstis, 1990) and enables

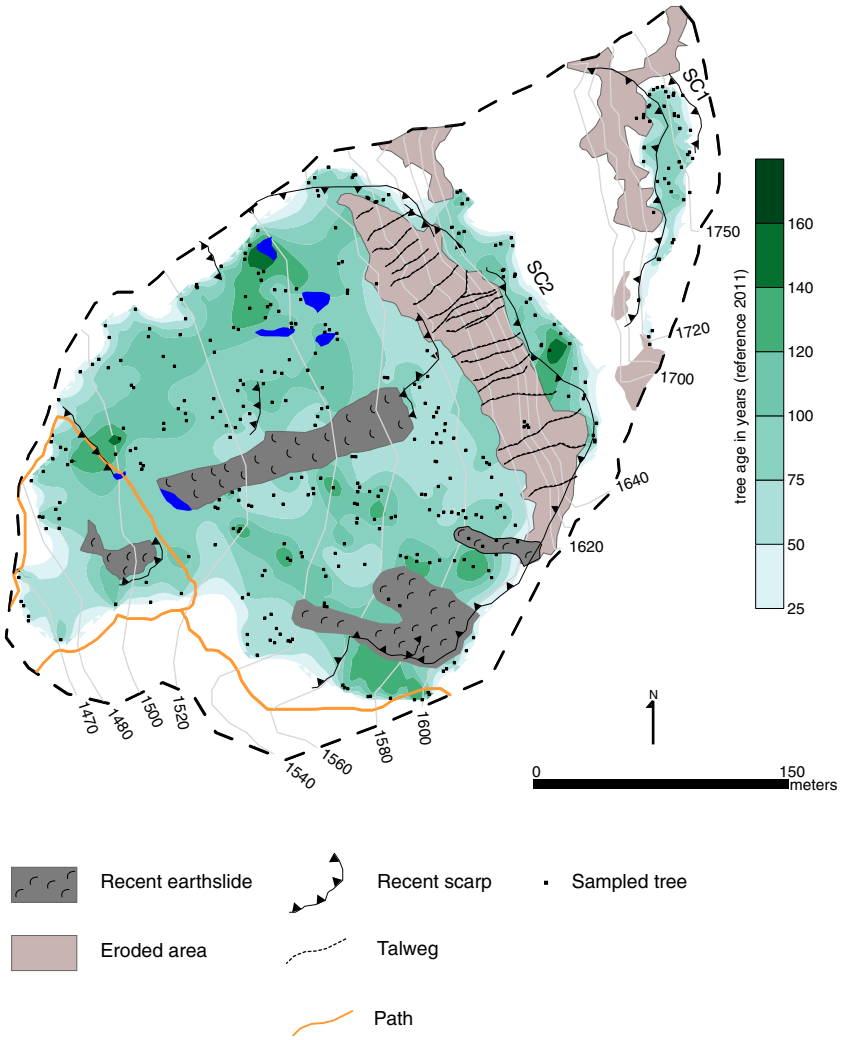

Fig. 3. Location and mean age of the 350 *P. uncinata* Mill. Ex. Mirb trees sampled at the Pra Bellon landslide. Interpolation was performed using geostatistical analyst (ESRI, 2005) and inverse distance weighted method.

precise cross-dating and age correction of the cores sampled on the landslide body.

The samples obtained in the field were analyzed and data processed following standard dendrochronological procedures (Bräker, 2002; Stoffel and Bollschweiler, 2008). Single steps of surface analysis included sample mounting on a slotted mount, sample drying, and surface preparation by finely sanding the upper core surface up to grit size 600. In the laboratory, tree rings were counted and ring widths measured to the nearest 0.01 mm using a digital LINTAB positioning table connected to a Leica stereomicroscope and TSAP-Win Scientific software (Rinntech, 2009). The reference chronology was developed based on the growth curves of the undisturbed trees using the ARSTAN software (Cook, 1985). The two measurements of each reference tree were averaged, indexed, and detrended using a double detrending procedure (Holmes, 1994) with a negative exponential curve (or linear regression) and a cubic smoothing spline function (Cook and Kairiukstis, 1990). The quality of the cross-dating was evaluated using COFECHA (Holmes, 1983) as well as the graphical functions of TSAPWin (Rinntech, 2009). Growth curves of the samples of disturbed trees were then compared with the reference chronology to detect missing, wedging, or false rings and to identify reactions to mechanical stress. As no significant correlation was found between the reference chronology and 156 cores from 53 affected trees (13%), these trees were not considered for further analysis.

3.3. Sign of disturbance in the tree-ring record

Landslide movement induces several kinds of growth disturbances (GD) to trees, most commonly in the form of an abrupt reduction in annual ring width and/or the formation of compression wood on the tilted side of the stem. A reduction in annual ring width over several years is interpreted as damage to the root system, loss of a major limb, or a partial burying of the trunk resulting from landslide activity (Carrara and O'Neill, 2003). In this study, growth-ring series had to exhibit (i) a marked reduction in annual ring width for at least five consecutive years such that (ii) the width of the first narrow ring was 50% or less of the width of the annual ring of the previous year.

The onset of compression wood is interpreted as a response to stem tilting induced by landslide pressure. Tilted trees try to recover straight geotropic growth (Mattheck, 1993) through the development of asymmetric growth rings, i.e., formation of wider annual rings with smaller, reddish-yellow colored cells with thicker cell walls (so-called compression wood; Timell, 1986) on the tilted side and narrow (or even discontinuous) annual rings on the opposite side of the tree (Panshin and De Zeeuw, 1970; Carrara and O'Neill, 2003). Finally, the formation of callus tissue was interpreted as a reaction to the corrasion of tree stems by the debris that causes damage and scars (Hupp, 1983).

3.4. Age structure of the stand

The age structure of the stand was approximated by counting the number of tree rings of selected trees (87% of the sampled population) and visualized after an "inverse distance weighted" interpolation using ArcGIS 9.3 (ESRI, 2005). Interpolations were performed using an ellipse-shaped search including data from 10 to 15 neighboring weighted points within each of its four sectors. The same method was used for the return period and probability maps.

However, because trees were not sampled at their stem base and the piths or innermost rings of several trees were rotten, the age structure is biased and does not reflect inception germination dates. Nonetheless, it provides valuable insights into major disturbance events at the study site with reasonable precision.

3.5. Dating of events

Determination of events was based on the number of samples showing GD in the same year and on the distribution of affected trees on the landslide body (Bollschweiler et al., 2008). To avoid overestimation of GD within the tree-ring series in more recent years because of the larger sample of trees available for analysis, we used an index value (I_t) as defined by Shroder (1978) and Butler and Malanson (1985):

$$I_t = \left(\sum_{i=1}^{n} (R_t) / \sum_{i=1}^{n} (A_t) \right) \times 100 \quad (1)$$

where R is the number of trees showing a GD as a response to a landslide event in year t, and A is the total number of sampled trees alive in year t. Following disturbance by an initial event, a tree may not necessarily yield useful data on additional events for some time (i.e., a tree may already be forming a narrow band of annual rings such that a subsequent disturbance would not be detected); this is why I was adjusted to only take account of trees with a useful record for year t (Carrara and O'Neill, 2003).

In this study, a minimum of 10 trees exhibiting a response (e.g., Dubé et al., 2004; Corona et al., 2010) was required for an event to be dated so as to avoid an overestimation of relative response numbers resulting from a low number of trees early in the record (e.g., Dubé et al., 2004). In order to minimize the risk that GD caused by other (geomorphic) processes could mistakenly be attributed to a landslide event and to take into account the sampling size, the chronology of past events was also based on $It \geq 5\%$.

However, the strictness of these thresholds and the large sample size may induce a misclassification of minor events. To avoid misclassification, the yearly patterns of disturbed trees for years with $2\% \geq It < 5\%$ and GD in at least five trees were carefully examined. Using geographical coordinates, trees were placed into a geographical information system (GIS; ArcGIS 9.3; ESRI, 2005) as geo-objects, and years of GD were linked as attributes to each single tree. We computed autocorrelations (feature similarity) based on the location and values of trees with the ArcGIS pattern analysis module (ESRI, 2005) and calculated yearly Moran indices (Moran, 1950) to evaluate whether the pattern of disturbed trees was clustered, dispersed, or random. A Moran index value near 1 indicates clustering, while a value near −1 indicates dispersion. The Z scores and p-values were used to indicate the significance of individual Moran index values. Random and dispersed patterns were disregarded from the reconstruction, whereas years with clustered patterns were considered as minor or spatially limited events.

3.6. Calculation of landslide return periods and probabilities of reactivation

Traditionally, the return period designates the mean time interval at which a material reaches a given point in an avalanche path (McClung and Schaerer, 1993; Corona et al., 2010). Frequency is usually expressed in years as a 'return period' (i.e., 1/frequency). By analogy, individual tree return periods (Rp) were calculated for the Pra Bellon landslide from GD frequency f for each tree T as follows (Reardon et al., 2008):

$$f_T = GD_T / A_T \quad (2)$$

where GD represents the number of growth disturbances detected in the tree T, and A the total number of years tree T was alive. Because of the exhaustive sampling and effectiveness of the dendrogeomorphic reconstruction, this approach was adapted to determine landslide return period.

Complete landslide records covering a long timespan may be used to perform probabilistic analyses (Corominas and Moya, 2008). The theoretical probability of a landslide to occur at Pra Bellon was modeled using a Poisson distribution (Crovelli, 2000; Guzzetti, 2000; Corominas and Moya, 2008). This model was applicated to many other hazard processes besides landslides, for example, earthquakes, floods, tsunamis, volcanoes, and storms (Crovelli, 2000). The Poisson model allows determination of future landslide probability based on the assumption (Guzzetti et al., 2005) that (i) the number of landslide events that occurs at disjoint time intervals is independent; (ii) the probability of an event occurring in a very short time is proportional to the time interval; (iii) the probability of more than one event in a short time interval is negligible; (iv) the probability distribution of the number of events is the same for all time interval of fixed lengths; and (v) the mean recurrence of events will remain the same in the future as it was observed in the past. Based on the above consideration, the probability (p) for an event with a return period (T) to occur in a given number of years N (fixed to 5, 10, 20, and 100 years) was computed as follows:

$$p = 1 - \mathrm{Exp}(-N/T). \quad (3)$$

According to this distribution, the probability P for a centennial event to occur during the next 100 years is, for example, 0.63.

4. Results

4.1. Age structure of the stand and growth disturbances

Pith age data from 350 *P. uncinata* trees sampled at Pra Bellon suggest an average age of the sample of 91 ± 28 years. Only one-third of the trees (32%) is older than 100 years with the oldest tree selected for analysis showing its first ring at sampling height in 1848; the youngest tree reached sampling height in 1983. As can be seen in Fig. 3, the distribution of tree ages is heterogeneous and the forest matrix is constituted by trees aged between 50 and 100 years with patches of old trees (>120 years) scattered within the matrix. According to the tree-ring data, individual old trees were present since the mid-nineteenth century and progressively colonized the landslide body.

A total of 704 GD related to a past landslide event was identified in the 350 *P. uncinata* trees. The most common reaction to landslide events was in the form of abrupt growth reductions with 63% of all GD (448 GD). The onset of compression wood (222 GD, 31%)

Table 1
Yearly Moran Indices and corresponding patterns computed for years with 5%>*It*>2% and GD>5.

Year	Moran's index	Distribution
1881	−0.03	Dispersed
1907	0.05	Dispersed
1911	0.14	Clustered
1919	0.21	Clustered
1921	0.13	Clustered
1925	0.02	Dispersed
1940	0.14	Clustered
1942	0.06	Dispersed
1946	−0.01	Dispersed
1951	0.01	Dispersed
1955	−0.01	Dispersed
1960	−0.01	Dispersed
1993	0.13	Clustered

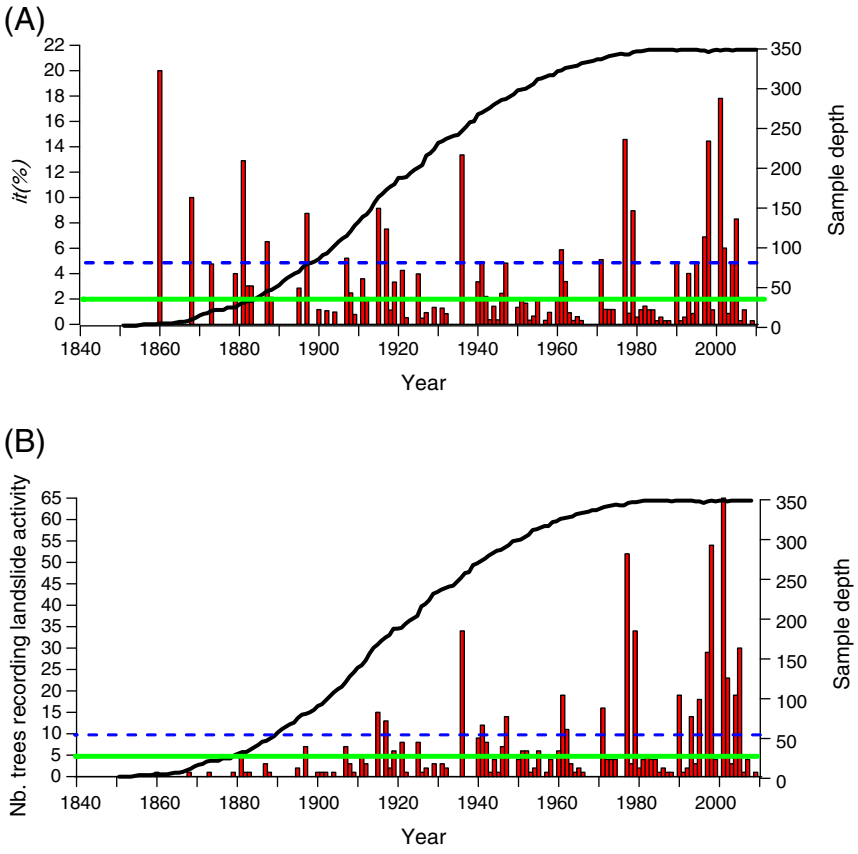

Fig. 4. Event response histograms showing landslide-induced growth disturbances (GD) from sampled trees. (A) Percentage of trees and (B) total number of trees responding to a damage event. Blue (green) horizontal dotted lines demarcates in (A) the 5% (2%) sample depth thresholds, and in (B) the n = 10 (n = 5) tree threshold. The black line shows the sample depth (i.e., the total number of trees alive in each year).

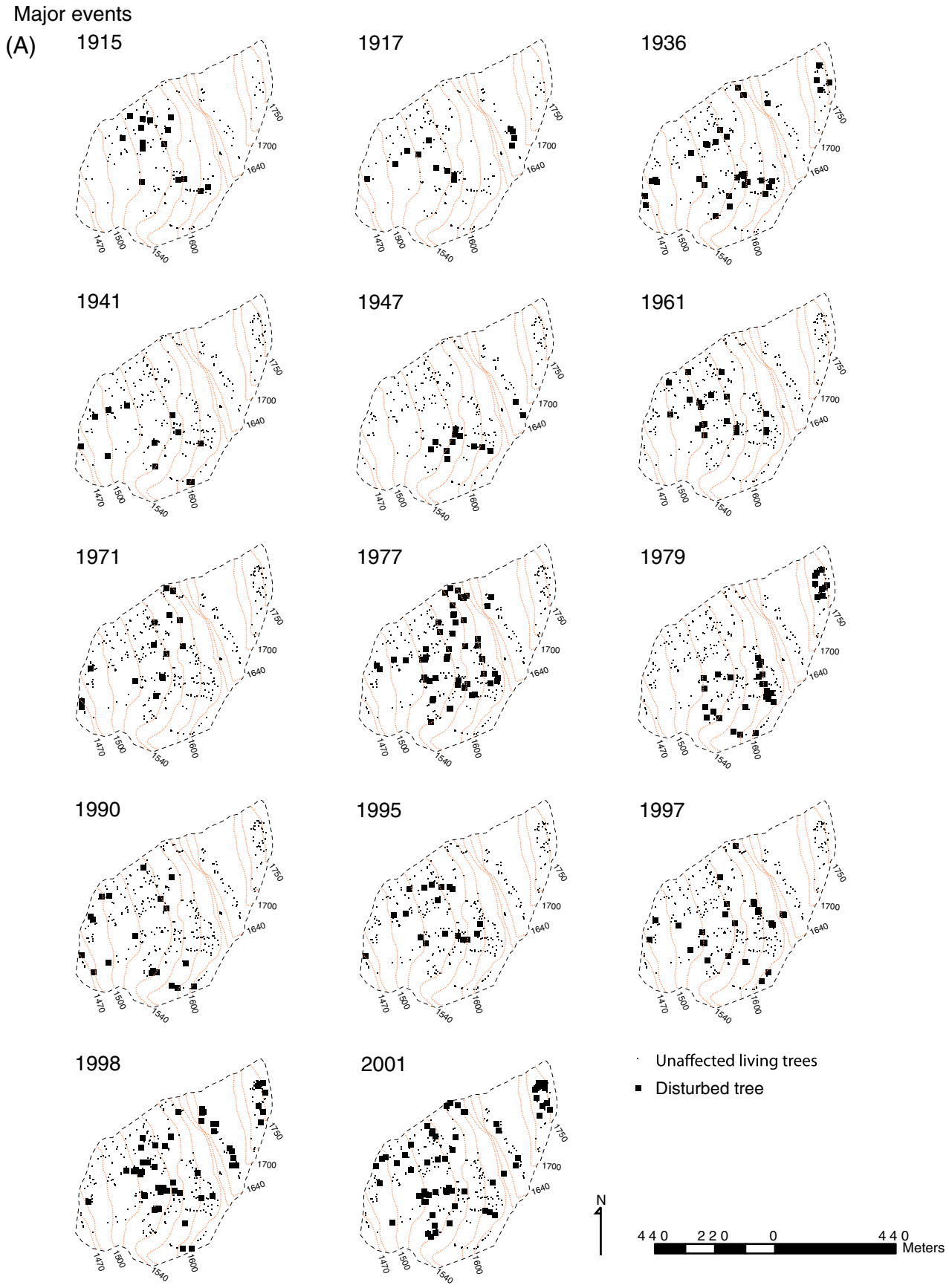

Fig. 5. Event-response maps showing the Pra Bellon landslide for each of the reconstructed reactivation events. Large dots indicate trees disturbed by the mass movement; small dots represent trees that are alive but not affected by the reactivation.

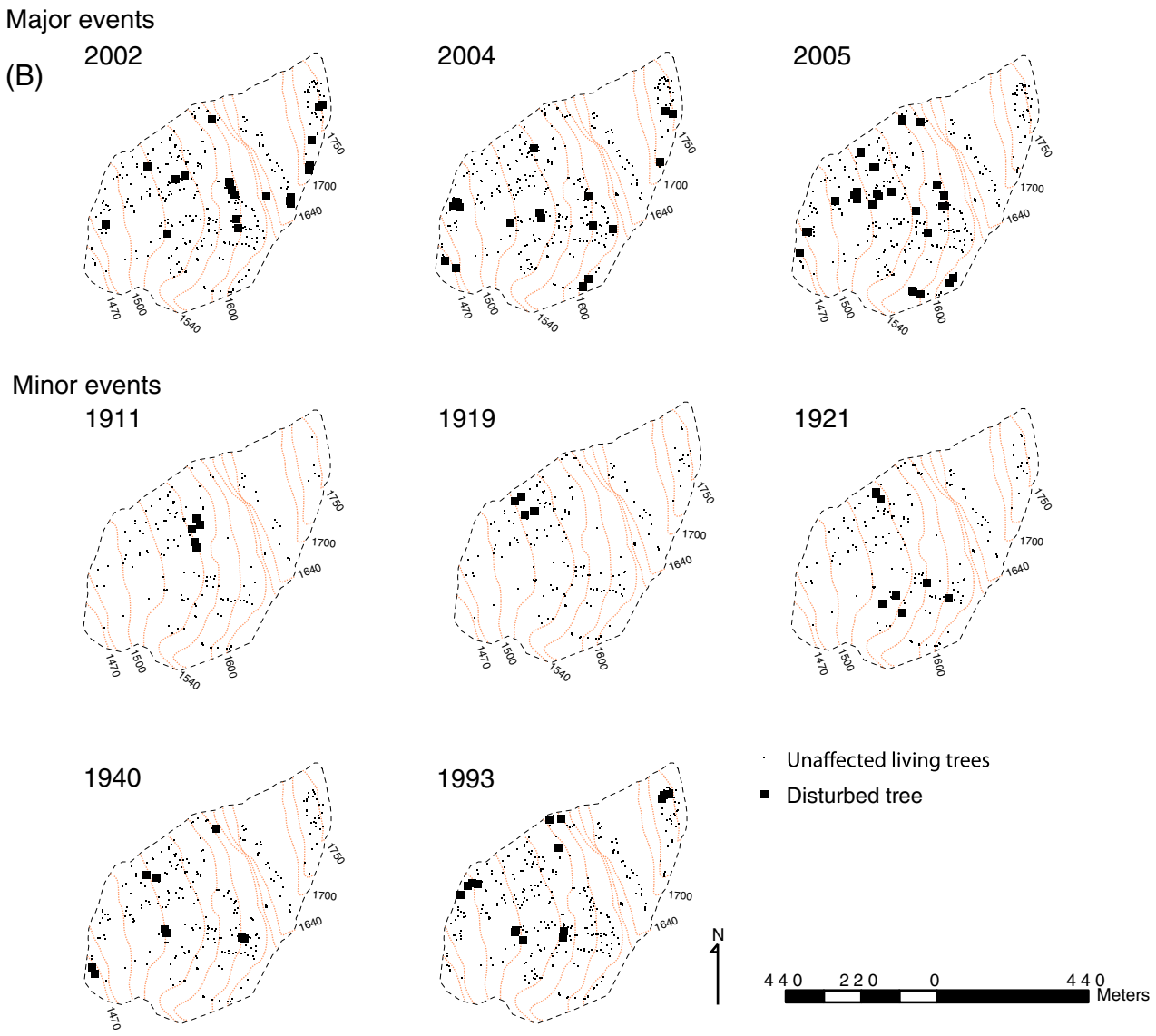

Fig. 5 (*continued*).

represents another common response of *P. uncinata* to landsliding. In contrast, the formation of callus tissue (34 GD) was by far less abundant. The earliest GD observed in the tree-ring series dates back to 1860; however, this year was not considered a landslide event as only two trees showed GD (Figs. 4A,B). In 1881, the number of GD surpassed five which was defined the threshold for GD to be considered as a landslide event.

4.2. Landslide events and decadal landslide frequency

The 704 GD identified in the tree-ring series allowed dating of 22 landslide events between 1911 and 2005. As can be seen in Fig. 4, the dating of 17 events (1915, 1917, 1936, 1941, 1947, 1961, 1971, 1977, 1979, 1990, 1995, 1997, 1998, 2001, 2002, 2004, and 2005) was based on $It \geq 5\%$ and GD in at least 10 trees. In contrast, for the events dated to 1881, 1907, 1911, 1919, 1921, 1925, 1940, 1942, 1946, 1951, 1955, 1960, and 1993, the limited number of GD was >5 and $5\% > It > 2\%$ did not allow for them being considered events with equal confidence. The yearly Moran I statistics computed for these years vary between −0.03 in 1881 (i.e., dispersed distribution of affected trees) and 0.21 in 1919 (i.e., spatial clustering of GD). Only 5 of these events (1911, 1919, 1921, 1940, and 1993) display clustered patterns of disturbed trees with sufficient aggregation to be considered landslide events (Table 1). In 1881, 1907, 1925, 1942, 1946, 1951, 1955, and 1960, the spatial distribution of disturbed trees does not display any significant pattern and these years were not therefore kept for further analysis.

Determination of decadal variations in landslide frequency at Pra Bellon was limited to the twentieth and twenty-first centuries where the number of trees and data coverage were sufficient. The mean number of events per decade amounts to 2 with a range from 0 (1900–1909, 1950–1959, and 1980–1989) to 5 (1990–2000). The recent part of the record (1990–2010) exhibits a very pronounced activity with 9 events. The periods 1921–1936, 1961–1971, and 1979–1990 represent phases of reduced landslide activity with no events reconstructed based on the dendrogeomorphic record.

4.3. Spatial distribution of trees disturbed by landslide events

Event-response maps are provided in Fig. 5 and yielded four distinct patterns for landslide events at Pra Bellon. The landslides dated to 1936, 1979, 1998, 2001, 2002, and 2004 represent event pattern 1 and covered the entire study areas including trees located on SC1. Event pattern 2 is represented with landslide events of 1961,

1977, 1990, 1997, and 2005. Here, only trees located in the main landslide body were affected by instability. Event pattern 3 is illustrated with the events of 1915, 1917, 1941, 1947, 1971, and 1995 and characterized by tree disturbance in well-defined and isolated segments of the landslide body (<0.2 ha) and correspond to years defined as minor events in the previous section. For instance, the event of 1947 only disturbed trees located in the southeastern part of the landslide body. In a similar way, the event of 1940 caused 9 GD, an *It* = 4%, and affected at least two trees each in four distinct landslide segments with surfaces ranging from 0.05 to 0.12 ha.

4.4. Return period and landslide probability maps

Considering the 22 reconstructed events within the sampled area, the mean return period for the Pra Bellon landslide is 4.5 years (median: 2 years) for the period 1910–2011. When analyzed spatially, the return period shows a clear increase from the central part (6 years) to the margins (>80 years) of the landslide body (Fig. 6A). When younger trees (<100 years) are excluded from the interpolation (Fig. 6B), return periods increase from 14 years on both sides of the recent earthflow to >100 years at the margins of the landslide body. However, the same patterns are observed in both maps revealing that increase of return periods toward the margins of the landslide body is independent of tree age.

Return periods of landslide were transformed into landslide occurrence probability using a Poisson distribution. Highly resolved maps of return period derived from the 350 cross-dated *P. uncinata* trees were then used to represent the probability for a landslide reactivation to occur within 5, 20, 50, and 100 years (Fig. 7A–D). As expected, the probability for a landslide to be reactivated is highest in the central part of the landslide body and increases from 0.13 for a 5-year period to 0.94 for a 100-year period. At the margins, the probabilities for an event are lower, yet they remain >0.6 for the 100-year period.

5. Discussion

Dendrogeomorphic analysis of 1563 increment cores taken from 403 *P. uncinata* allowed reconstruction of 22 events for the Pra Bellon landslide between 1910 and 2011. The reconstruction added 21 previously unknown events to the historic chronology and confirmed the event of 1971 known from archival records (Delsigne et al., 2001).

The reconstructed time series represents a minimum frequency of reactivation events for the Pra Bellon landslide in the recent past as the reconstruction was limited by tree age. The 'état-major' topographical map (Fig. 8A), realized between 1825 and 1866, does not show a continuous forest in the Pra Bellon area and therefore supports our data suggesting tree germination and the establishment of a forest at the study site in the second half of the nineteenth century. Furthermore, the existence of SC2 on the 'état-major' map reveals that the first occurrence of landslides at Pra Bellon predates the first event reconstructed with dendrogeomorphic techniques to 1911. The first event in our record therefore represents a reactivation and not an initial landslide event.

Several limitations are apparent as to the potential of tree-ring analysis to detecting past periods of landslide activity. Reactivation of the landslide body must be, on one hand, powerful enough to damage a sufficiently large number of trees through stem topping, tilting, or root damage. At the same time, more violent and destructive events are likely to kill trees and evidence of this category of events is not likely to be available to the investigator, as dead trees will disappear some time after an event.

Despite these limitations, the methodology deployed in this study enhances the reliability of datasets on past landslide events at the local level. In addition, the *It* and GD thresholds as well as the spatial analysis of event-response maps minimized the risk of GD resulting from nonlandslide events to be included in the chronology. The thresholds also allowed rejection of GD related to creep or fall that have been shown to affect a rather limited number of trees per event (Stoffel and Perret, 2006).

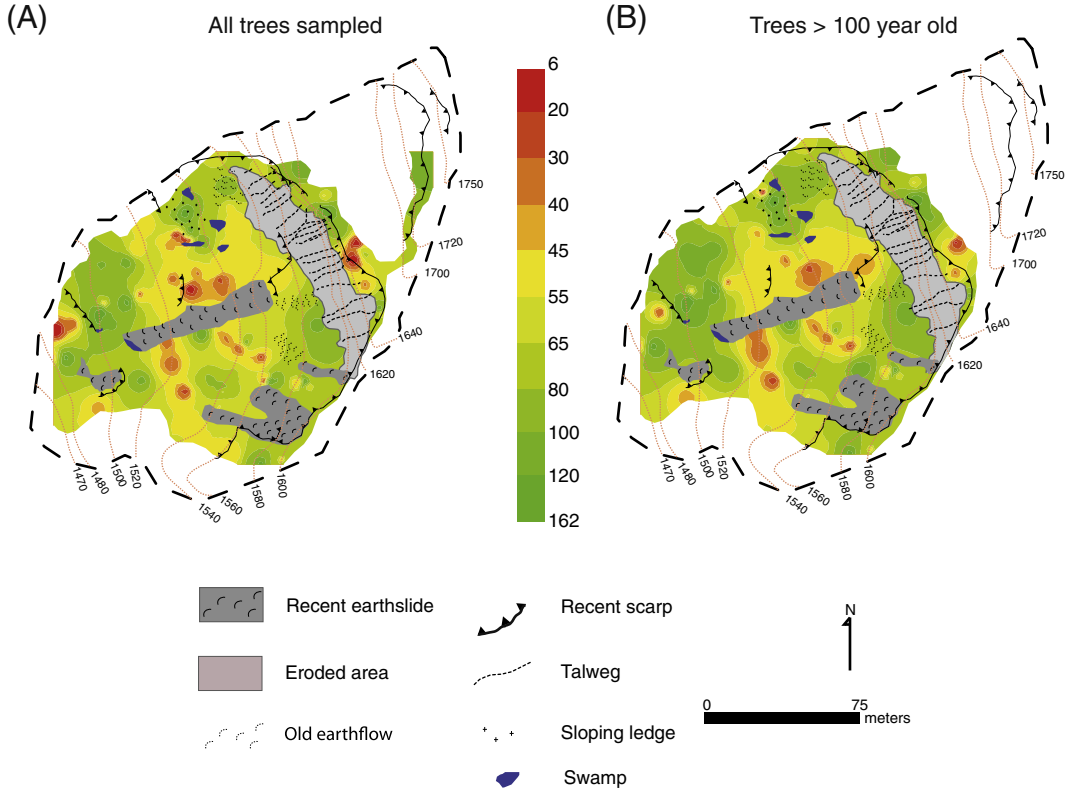

Fig. 6. Interpolated return periods for the sampled area of the Pra Bellon landslide. Return period maps were computed with (A) the whole sampled trees and (B) only trees aging at least 100 years for the period 1910–2011.

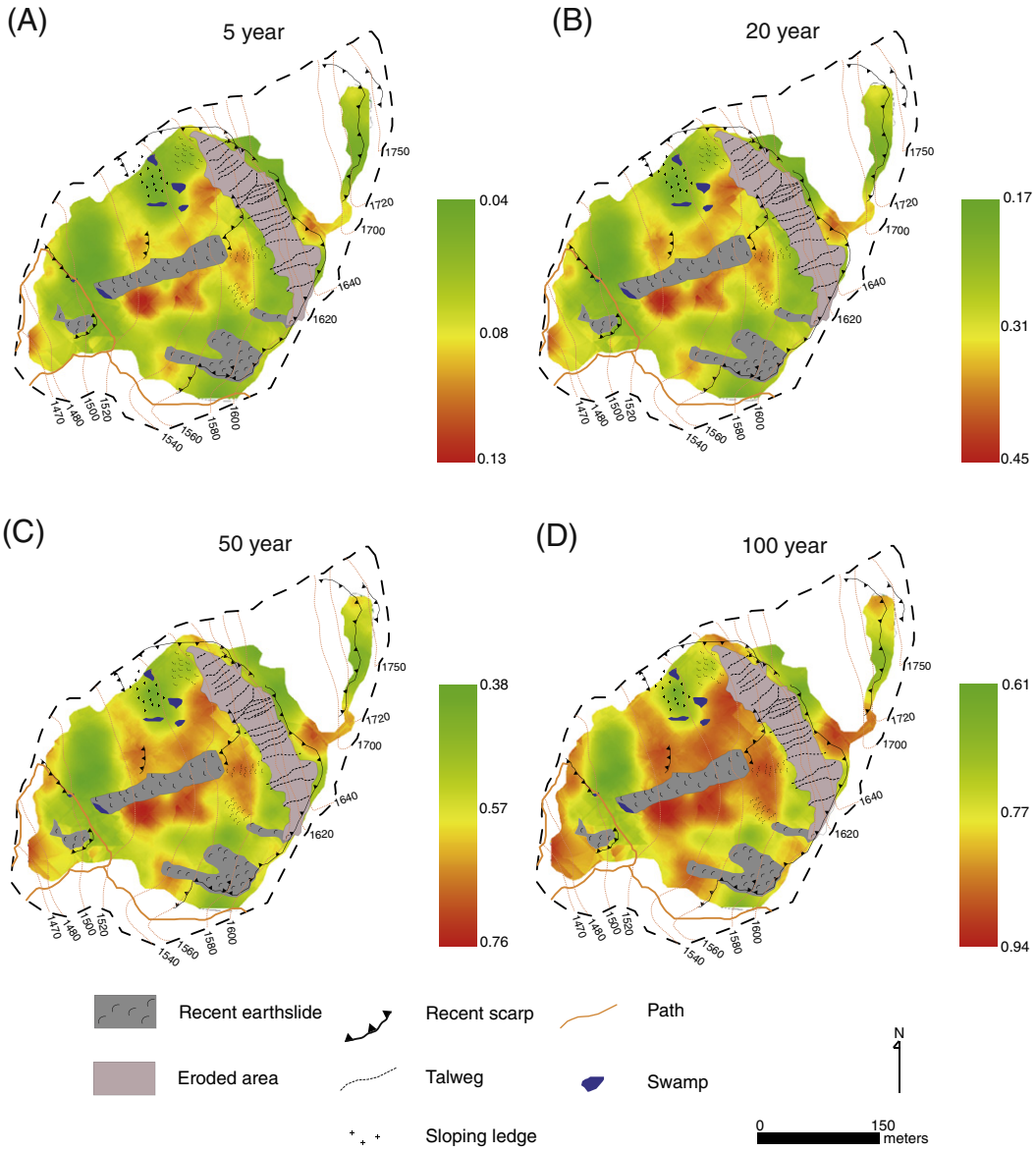

Fig. 7. Probability maps of reactivation for the Pra Bellon landslide within (A) 5, (B) 20, (C) 50 and, (D) 100 years computed using a Poisson distribution model.

For the period 1948–2007, the diachronic analysis of aerial photographs provides additional evidence for the spatiotemporal accuracy of the dendrogeomorphic reconstruction presented in this paper. The reactivations of 1961 and 1971, deciphered from the tree-ring records, are supported by the slight extension of bare areas observed in the landslide body and by a local slide in the northwestern part of SC2 between 1948 (Fig. 8B) and 1974 (Fig. 8C). Between 1974 and 1982 (Fig. 8D), the diachronic analysis suggests significant changes with several bare areas downslope of SC1 or within the landslide body. These changes thus support the assumption of two major events reconstructed in 1977 and 1979. Between 1982 and 1995 (Fig. 8E), an earthslide destroyed a large part of the forest stand in the southeastern part of the landslide body. Interestingly, a unique event is reconstructed for this period and dated to 1990. The GD of this landslide are observed in several trees growing at the periphery of this slide. Similarly, the earthslide observed in the western part of the landslide body between 2000 (Fig. 8F) and 2007 (Fig. 8G) corroborates the event-response map reconstructed for an event in 2001.

Fig. 9 shows a comparison of our reconstructed landslide events (Fig. 9A) with historical archives (i) of debris flows in the Riou Bourdoux catchment (1910–1994, Fig. 9B) and (ii) landslide events in the wider Barcelonnette region (1910–2003, Fig. 9C). The historical archive of debris flows in the Riou Bourdoux catchment (Delsigne et al., 2001) contains 29 events in 18 distinct years between 1910 and 1994 and suffer from a major gap during the interwar period (1918–1947). Only four years coincide between the two records, namely 1915, 1917, 1977, and 1979 (Figs. 9A,B). Conversely, five landslide events are not synchronous with debris-flow activity in the Riou Bourdoux catchment, and 14 debris flows do not have any analogs with reconstructed landslides. Although precipitation certainly plays a crucial role in the triggering of both processes, intense rainfalls capable of generating debris flows in the Riou Bourdoux

Fig. 8. Diachronic evolution of the Pra Bellon landslide between 1825 and 2007. (A) Etat Major topographical map and aerial photographs of the landslide area in (B) 1948 (National Geographic Institute, IGN aerial mission, 1948_F3537-3540_P30000), (C) 1974 (1974_FR2620_P_110000), (D) 1982 (1982_IFN04_P_17000), (E) 1995 (1995_F3539-3540_P30000), (F) 2000 (2000_FD04_C_25000), and (G) 2007 (IGN special mission for the Riou Bourdoux catchment). The dashed line indicates the investigated area and the white arrow shows the landslide movements.

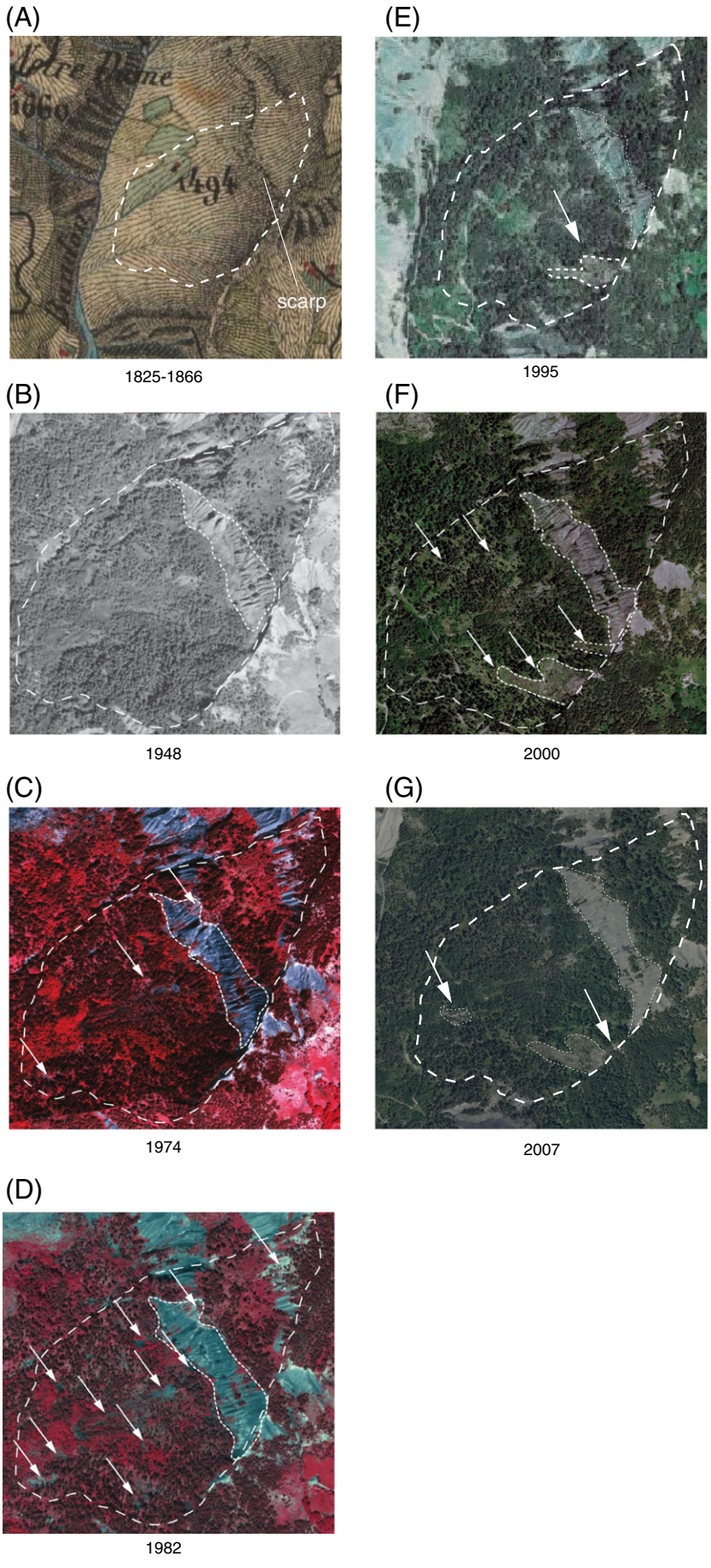
(A)
scarp
1825-1866
(E)
1995
(B)
1948
(F)
2000
(C)
1974
(G)
2007
(D)
1982

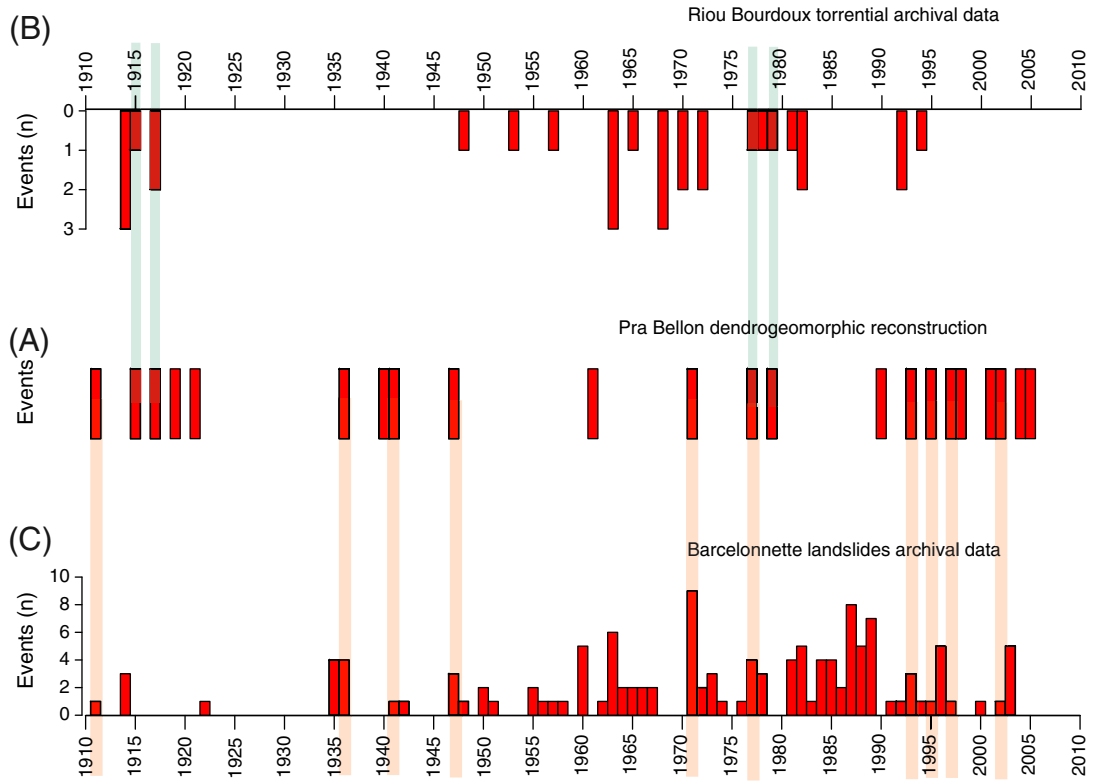

Fig. 9. Comparison of (A) the dendrogeomorphic reconstruction with (B) the Riou-Bourdoux torrential archival data and (C) the regional archives of landsliding in the Barcelonnette basin for the common period 1910–2010. Gray (brown) shaded bars indicate coincidence between the reconstruction and the Riou Bourdoux (regional) archives.

catchment (Remaître, 2006) will not necessarily be sufficient to cause the Pra Bellon landslide to reactivate.

Additionally, the dendrogeomorphic time series of landslides was compared with archival records on landslides in the Barcelonnette area (Amiot and Nexon, 1995; Flageollet, 1999). This continuous record contains 138 historical references to shallow landslides and mudslides. For sites located in the vicinity of the Pra Bellon landslide, isolated events have been inventoried for 1911, 1941, 1995, 1997, and 2002; landslide activity at three locations in 1936, 1947, and 1993; at four sites in 1977; and even on nine different landslide bodies in 1971 (Fig. 9A,C). When compared with the reconstructed Pra Bellon series, analogs cannot be found for 12 dates (namely 1915, 1917, 1919, 1921, 1940, 1961, 1979, 1990, 1998, 2001, 2004, and 2005) and therefore remain unconfirmed. If the comparison is done at the decadal scale, a complete absence of events can be observed at the local (Pra Bellon) and regional scales between 1922 and 1935. For the period 1980–1990, the Pra Bellon reconstruction shows a complete absence of landslides whereas an increase in landslide frequency is observed at the regional scale, partly related to the triggering of mudslides at La Valette and Super Sauze (Malet, 2003).

The reconstruction of spatiotemporal patterns of landslide activity with dendrogeomorphic techniques is recent but has been helpful for the understanding of landslide kinematics and its spatial evolution (Corominas and Moya, 2010). Fantucci and McCord (1995), for instance, identified reactivation events of a landslide at Fossatello between 1880 and 1994 and produced maps showing parts of the landslide body reactivated in 10-year periods. In our study, the exhaustive sampling of *P. uncinata* trees allowed computation of a very detailed spatiotemporal chronology of landslide reactivation at Pra Bellon. Given the completeness of the reconstruction (since 1910), we were able to map return periods of reactivation. Assuming that landslide recurrence will remain comparable in the future, and adopting a Poisson probability model (Guzzetti et al., 2005), we were also able to determine the probability of having a reactivation in each mapping unit for time intervals varying from 5 to 100 years. Highest return periods associated with major probabilities of reactivation are mapped in the central part of the landslide body on each side of a recent earthslide. Despite forest restoration efforts in the basin, our data illustrates that the return period of landslides at Pra Bellon sharply increased over the last 50 years.

Our approach purposely does not include physically based modeling, as this conventional method has been shown to predict the spatiotemporal occurrence of landslides with difficulties (Jaiswal et al., 2011). Most previous work focusing on landslide mapping has been based on susceptibility maps and therefore provides an estimate of where landslides are expected to occur (e.g., Brabb, 1984; Guzzetti et al., 2005). Much less work has been done on the establishment of the temporal probability of reactivation (Coe et al., 2000; Guzzetti et al., 2005). The approach presented in this paper allows determination of quantitative probabilities of reactivation estimated directly from the frequency of past landslide events and does not require a landslide susceptibility analysis as a complete inventory of past landslide events was reconstructed with dendrogeomorphic techniques (Corominas and Moya, 2008).

However, it is based on the Poisson probability model which among others assumptions are: (i) the number of events which occur in one time interval or region of space are independent of the number that occurs in any other disjoint time interval or region; (ii) the probability distribution of the number of events remains the same for all time intervals of a fixed length. In reality, most hazardous events, including landslides, are probably not independent and do not occur at random (Coe et al., 2000). For example, the reactivation of a landslide may make the landslide more or less susceptible to future landslides, thus creating stability or instability in the future. Also, changing land use, local changing climatic conditions or implementation of landslide mitigation measure may consequently make the

occurrence of landslides more or less likely in the future (Chleborad et al., 2006). Nevertheless, the Poisson model is often used when no information other than the mean rate of event occurrence is known. Under such circumstances, the Poisson model provides a good first-cut estimate for the probability of event occurrence in the future (Coe et al., 2000).

6. Conclusion

Because of increased activity in mountain areas, it has become imperative to improve landslide forecasting at the local scale, which is currently difficult using statistical analysis or physically-based models. In this study, we demonstrate the potential of extensive dendrogeomorphic analyses to add substantially to the spatiotemporal record of landslides at a study site. In addition, dendrogeomorphic data have also been shown to add very accurate evidence to the extent of past reactivation and could efficiently complement other conventional methods. For land use planning, the identification of endangered areas is of paramount, importance and dendrogeomorphic mapping should therefore be used systematically for hazard zoning in forested areas affected by shallow landslides. Finally, if coupled with a Poisson model, dendrogeomorphic mapping can improve our knowledge about the probability of reactivation. These probability maps should be used for disaster prevention and generation of risk maps, as well as for the detailed design phase of engineering works and for the construction of slope stabilization works.

Acknowledgments

This research has been supported by the DENDROGLISS program, funded by the MAIF Foundation and the Cemagref by the PARAMOUNT program, 'ImProved Accessibility, Reliability and security of Alpine transport infrastructure related to MOUNTainous hazards in a changing climate', funded by the Alpine Space Programme, European Territorial Cooperation, 2007–2013. It has also been supported by the EU-FP7 project ACQWA (project no. GOCE-20290). The authors would like to acknowledge R. Marston and three journal reviewers whose insightful comments helped them improve an earlier version of the paper.

References

Aleotti, P., Chowdhury, R., 1999. Landslide hazard assessment: summary review and new perspectives. Bulletin of Engineering Geology and the Environment 58, 21–44.
Alestalo, J., 1971. Dendrochronological interpretation of geomorphic processes. Fennia 105, 1–139.
Alexander, D., 2008. A brief survey of GIS in mass-movement studies, with reflections on theory and methods. Geomorphology 94, 261–267.
Amiot, A., Nexon, C., 1995. Inventaire des aléas dans le Bassin de Barcelonnette depuis 1850. Mémoire de Maîtrise de Géographie Physique. Université Louis Pasteur, Strasbourg, France. 173 pp.
Antoine, P., 1995. Geological and geotechnical properties of the Terres noires in southeastern France: weathering, erosion, solid transport and instability. Engineering Geology 40, 223–234.
Astrade, L., Bravard, J., Landon, N., 1998. Mouvements de masse et dynamique d'un géosystème alpestre : étude dendrogéomorphologique de deux sites de la valle de Boulc (Diois, France). Géographie Physique et Quaternaire 52, 153–166.
Bégin, C., Filion, L., 1988. Age of landslides along the grande rivière de la Baleine estuary, Eastern coast of Hudson bay, Québec (Canada). Boreas 17, 289–299.
Bollschweiler, M., Stoffel, M., Schneuwly, D., 2008. Dynamics in debris-flow activity on a forested cone a case study using different dendroecological approaches. Catena 72, 67–78.
Braam, R., Weiss, E., Burrough, P., 1987. Spatial and temporal analysis of mass movement using dendrochronology. Catena 14, 573–584.
Brabb, E., 1984. Innovative approaches to landslide hazard mapping. Proceedings of 4th International Symposium on Landslides. Canadian Geotechnical Society, Toronto, Canada, pp. 307–323.
Bräker, O., 2002. Measuring and data processing in tree-ring research? A methodological introduction. Dendrochronologia 20, 203–216.
Brunsden, D., Jones, D.K.C., Arber, M.A., 1976. The evolution of landslide slopes in Dorset. Philosophical Transactions of the Royal Society of London. Series A: Mathematical and Physical Sciences 283, 605–631.
Butler, D.R., 1979. Dendrogeomorphological analysis of flooding and mass movement, Ram Plateau, Mackenzie Mountains, northwest Territories. The Canadian Geographer. doi:10.1111/j.1541-0064.1979.tb00638.x.
Butler, D.R., Malanson, G.P., 1985. A history of high-magnitude snow avalanches, southern Glacier National Park, Montana, U.S.A. Mountain Research and Development 5, 175–182.
Caris, J., van Asch, T., 1991. Geophysical, geotechnical and hydrological investigations of a small landslide in the French Alps. Engineering Geology 31, 249–276.
Carrara, P., O'Neill, J.M., 2003. Tree-ring dated landslide movements and their relationship to seismic events in southwestern Montana, USA. Quaternary Research 59, 25–35.
Carrara, A., Crosta, G., Frattini, P., 2003. Geomorphological and historical data in assessing landslide hazard. Earth Surface Processes and Landforms 28, 1125–1142.
Chleborad, A.F., Baum, R.L., Godt, J.W., 2006. Rainfall Thresholds for Forecasting Landslides in the Seattle, Washington, Area-Exceedance and Probability. USGS Open-File Report 2006–1064.
Claessens, L., Verburg, P.H., Schoorl, J.M., Veldkamp, A., 2006. Contribution of topographically based landslide hazard modelling to the analysis of the spatial distribution and ecology of Kauri (*Agathis australis*). Landscape Ecology 21, 63–76.
Coe, J., Michael, J., Crovelli, R., Savage, W., 2000. Preliminary map showing landslide densities, mean recurrence intervals, and exceedance probabilities as determined from historic records, Seattle, Washington. USGS Open-file Report 00-0303. Available at http://pubs.usgs.gov/of/2000/ofr-00-0303/.
Cook, E., 1985. A time series analysis approach to tree-ring standardization. Ph.D. thesis, University of Arizona, Tucson.
Cook, E., Kairiukstis, L., 1990. Methods of Dendrochronology: Applications in the Environmental Science. Kluwer Academic Publishers, International Institute for Applied Systems Analysis, Dordrecht, Netherlands.
Corominas, J., Moya, J., 1999. Reconstructing recent landslide activity in relation to rainfall in the Llobregat River basin, eastern Pyrenees, Spain. Geomorphology 30, 79–93.
Corominas, J., Moya, J., 2008. A review of assessing landslide frequency for hazard zoning purposes. Engineering Geology 102, 193–213.
Corominas, J., Moya, J., 2010. Contribution of dendrochronology to the determination of magnitude frequency relationships for landslides. Geomorphology 124, 137–149.
Corona, C., Rovéra, G., Lopez Saez, J., Stoffel, M., Perfettini, P., 2010. Spatio-temporal reconstruction of snow avalanche activity using tree rings: Pierres Jean Jeanne avalanche talus, massif de l'Oisans, France. Catena 83, 107–118.
Crovelli, R.A., 2000. Probability models for estimation of number and costs of landslides. USGS Open-File Report 00-249. USGS, Denver, CO.
Dehn, M., Buma, J., 1999. Modelling future landslide activity based on general circulation models. Geomorphology 30, 175–187.
Delsigne, F., Lahousse, P., Flez, C., Guiter, G., 2001. Le Riou Bourdoux: un "monstre" alpin sous haute surveillance. Revue Forestière Française 527–541.
Dubé, S., Filion, L., Hétu, B., 2004. Tree-ring reconstruction of high-magnitude snow avalanches in the northern Gaspé Peninsula, Québec, Canada. Arctic, Antarctic, and Alpine Research 36, 555–564.
Efthymiadis, D., Jones, P.D., Briffa, K.R., Auer, I., Böhm, R., Schöner, W., Frei, C., Schmidli, J., 2006. Construction of a 10-min-gridded precipitation data set for the greater alpine region for 1800–2003. Journal of Geophysical Research. doi:10.1029/2005JD006120.
ESRI, 2005. ArcGIS 9.2. Redlands, CA.
Fantucci, R., McCord, A., 1995. Reconstruction of landslide dynamic with dendrochronological methods. Dendrochronologia 13, 43–58.
Fantucci, R., Sorriso-Valvo, M., 1999. Dendrogeomorphological analysis of a slope near Lago, Calabria (Italy). Geomorphology 30, 165–174.
Flageollet, J., 1999. Landslides and climatic conditions in the Barcelonnette and Vars basins (Southern French Alps, France). Geomorphology 30, 65–78.
Flez, C., Lahousse, P., 2003. Contribution to assessment of the role of anthropic factors and bioclimatic controls in contemporary torrential activity in the southern Alps (Ubaye valley, France). In: Elsevier (Ed.), The Mediterranean World, Environment and History, Paris, pp. 105–118.
Floris, M., Bozzano, F., 2008. Evaluation of landslide reactivation: a modified rainfall threshold model based on historical records of rainfall and landslides. Geomorphology 94, 40–57.
Fuller, M., 1912. The New Madrid Earthquake. Center for Earthquake Studies, Southeast Missouri State University, Cape Girardeau.
Guzzetti, F., 2000. Landslide fatalities and the evaluation of landslide risk in Italy. Engineering Geology 58, 89–107.
Guzzetti, F., Cardinali, M., Reichenbach, P., 1994. The AVI project: a bibliographical and archive inventory of landslides and floods in Italy. Environmental Management 18, 623–633.
Guzzetti, F., Reichenbach, P., Cardinali, M., Galli, M., Ardizzone, F., 2005. Probabilistic landslide hazard assessment at the basin scale. Geomorphology 72, 272–299.
Hilker, N., Badoux, A., Hegg, C., 2009. The Swiss flood and landslide damage database 1972–2007. Natural Hazards and Earth System Science 9, 913–925.
Holmes, R., 1983. Computer-assisted quality control in tree-ring dating and measurement. Tree-Ring Bulletin 44, 69–75.
Holmes, R., 1994. Dendrochronology Program Library — Users Manual. Laboratory of Tree-Ring Research, Tucson, Arizona, U.S.A.
Hovius, N., Stark, C.P., Allen, P.A., 1997. Sediment flux from a mountain belt derived by landslide mapping. Geology 25, 231.
Hupp, C.R., 1983. Geo-botanical evidence of late Quaternary mass wasting in block field areas of Virginia. Earth Surface Processes and Landforms 8, 439–450.
Ibsen, M., Brunsden, D., 1996. The nature, use and problems of historical archives for the temporal occurrence of landslides, with specific reference to the south coast of Britain, Ventnor, Isle of Wight. Geomorphology 15, 241–258.

Jaiswal, P., van Westen, C.J., Jetten, V., 2011. Quantitative assessment of landslide hazard along transportation lines using historical records. Landslides. doi:10.1007/s10346-011-0252-1.
Malet, J.P., 2003. Glissements de type écoulement dans les marnes noires des Alpes du Sud. Morphologie, fonctionnement et modélisation hydro-mécanique. Ph.D. thesis. Institut de Physique du Glober, Université Louis Pasteur. Strasbourg, France, pp. 364.
Maquaire, O., Malet, J.P., Remaître, A., Locat, J., Klotz, S., Guillon, J., 2003. Instability conditions of marly hillslopes: towards landsliding or gullying? The case of the Barcelonnette basin, south east France. Engineering Geology 70, 109–130.
Martin, Y., Rood, K., Schwab, J.W., Church, M., 2002. Sediment transfer by shallow landsliding in the Queen Charlotte Islands, British Columbia. Canadian Journal of Earth Sciences 39, 189–205.
Mattheck, C., 1993. Design in der Natur. Rom bach Wissenschaft, Reihe Okologie 1, 242.
McClung, D., Schaerer, P., 1993. The Avalanche Handbook. Mountaineers, Seattle, WA.
McGee, W.J., 1893. A fossil earthquake. Geological Society of America Bulletin 4, 411–414.
Meunier, M., Mathys, N., Cambon, J., 1995. Panorama synthétique des mesures d'érosion effectuées sur trois bassins du site expérimental de Draix. Technical Report. Cemagref, Grenoble, France.
Moran, P.A.P., 1950. Notes on continuous stochastic phenomena. Biometrika 37, 17–23.
Mulder, H., 1991. Assessment of landslide hazard. Ph.D. thesis, Faculty of Geographical Sciences, University of Utrecht, Netherlands, 149 pp.
Osterkamp, W., Hupp, C., Blodgett, J., 1986. Magnitude and frequency of debris flows, and areas of hazard on Mount Shasta, California. Geological Survey Professional Paper 1396-C, Vancouver, WA, p. 21.
Panshin, A., De Zeeuw, C., 1970. Textbook of Wood Technology 3e éd., McGraw-Hill, New York, USA.
Petrascheck, A., Kienholz, H., 2003. Hazard assessment and mapping of mountain risks in Switzerland. In: Rickenmann, D., Chen, C.L. (Eds.), Debris Flow Hazards Mitigation: Mechanics, Prediction and, Assessment. Millpress, Rotterdam, Netherlands, pp. 25–38.
Procter, E., Bollschweiler, M., Stoffel, M., Neumann, M., 2011. A regional reconstruction of debris-flow activity in the northern calcareous Alps, Austria. Geomorphology. doi:10.1016/j.geomorph.2011.04.035.
Reardon, B.A., Pederson, G.T., Caruso, C.J., Fagre, D.B., 2008. Spatial reconstructions and comparisons of historic snow avalanche frequency and extent using tree rings in Glacier National Park, Montana, U.S.A. Arctic, Antarctic, and Alpine Research 40, 148–160.
Reeder, J., 1979. The dating of landslides in Anchorage, Alaska. A case for earthquake triggered movements. Geological Society of America Abstracts with Programs, p. 501.
Remaître, A., 2006. Morphologie et dynamique des laves torrentielles : Applications aux torrents des Terres Noires du bassin de Barcelonnette (Alpes du Sud). Ph.D. Thesis, Département de Géographie Physique et Environnement, Université de Caen/Basse-Normandie, 487 p.
Rinntech, 2009. http://www.rinntech.com/content/blogcategory/2/28/lang,english.
Santilli, M., Pelfini, M., 2002. Dendrogeomorphology and dating of debris flows in the Valle del Gallo, central Alps, Italy. Dendrochronologia 20, 269–284.
Shroder, J., 1978. Dendrogeomorphological analysis of mass movement on Table Cliffs plateau, Utah. Quaternary Research 9, 168–185.
Stefanini, M., 2004. Spatio-temporal analysis of a complex landslide in the orthern Apennines (Italy) by means of dendrochronology. Geomorphology 63, 191–202.
Stien, D., 2001. Glissements de terrains et enjeux dans la vallée de l'Ubaye et le pays de Seyne. Rapport RTM, Barcelonnette, France. 218 pp.
Stoffel, M., Bollschweiler, M., 2008. Tree-ring analysis in natural hazards research — an overview. Natural Hazards and Earth System Science 8, 187–202.
Stoffel, M., Perret, S., 2006. Reconstructing past rockfall activity with tree rings: some methodological considerations. Dendrochronologia 24, 1–15.
Stoffel, M., Bollschweiler, M., Butler, D.R., Luckman, B., 2010. Tree Rings and Natural Hazards. Springer, Dordrecht, New York.
Thiery, Y., Malet, J., Sterlacchini, S., Puissant, A., Maquaire, O., 2007. Landslide susceptibility assessment by bivariate methods at large scales: application to a complex mountainous environment. Geomorphology 92, 38–59.
Timell, T., 1986. Compression Wood in Gymnosperms. Springer-Verlag, Berlin, New York.
Utasse, M., 2009. Cartographie morpho-dynamique et évolution historique de trois glissements actifs dans le basin versant du Riou-Bourdoux (Alpes-de-Haute-Provence, vallée de l'Ubaye). Mémoire de stage, Master 1, Géosciences, Environnement, Risques, Université de Strasbourg, France.
Van Den Eeckhaut, M., Muys, B., Loy, K.V., Poesen, J., Beeckman, H., 2009. Evidence for repeated re-activation of old landslides under forest. Earth Surface Processes and Landforms 34, 352–365.
Varnes, D.J., 1984. Landslide hazard zonation: a review of principles and practice. International Association of Engineering Geologists Comission on Landslides and Other Mass movements on Slopes. : Natural Hazards, 3. Unesco, Paris, p. 176.
Weber, D., 1994. Research into earth movements in the Barcelonnette basin. In: Casale, R., Fantechi, R., Flageollet, J.-C. (Eds.), Temporal Occurrence and Forecasting of Landslides in the European Community, Final Report 1, pp. 321–336.
Williams, P., Jacoby, G., Buckley, B., 1992. Coincident ages of large landslides in Seattle's Lake Washington. Geological Society of America Abstract with Programs, p. 90.